

Numerical Study of the Effect of Vertical Wind Break on the Trough Collector's Drag Force

Wisam Ahmed Abd Al-wahid

Ph.D. in Automobile Engineering Technology Department, Technical College-Najaf, Iraq

ABSTRACT: The effect of the addition of wind break wall upstream the wind flow is studied numerically. The separation distance between the trough and wind break, and the wind break elevation as well as the wind flow velocity will be the variables of the present work. The computational work done by use a 5.0 COMSOL Multiphysics code to solve the problem. The results show a general decrease in the drag forces on the trough as well as the heat loss. The extreme values of separation distance and wall elevation causes an opposite defect results.

KEYWORDS: Aerodynamic force, Turbulent flow, trough, wind break

I. INTRODUCTION

In developing solar collectors, wind loading is the major structural design consideration. Since the collectors work in the open field, they subjected to variant turbulent wind speeds continuously. The winds cause drag forces, which should be supported by the collectors' frame. The drag coefficient of a trough facing a wind is the worst case of drag force [1], but the value reduces to half if the wind reversed. Still, the values of drag forces are high and need to reduce. Many researchers studied the calculations of wind loading, since this field is still viral [2]. Some works reviewed previous researches and sum the results of these works for extreme benefits [2, and 3]. It found that the absorber's tube has no effect on the flow [4]. Therefore, the works focused on the trough to find the loads experimentally [5, 6, and 7], and numerically [4, 8, and 9].

Some researchers try to develop the shape of the trough to reduce the loads [4, and 8], and others by using a wall and fences [5, and 10]. The present work try to study, numerically, the effect of adding a wall put in front of the collector on the flow field and wind loading of the trough. Wind speed, and the separated distance are the variables of the study.

II. MATHEMATICAL MODEL

The equations used to solve the problem are the two-dimensional continuity equation, and Navier-Stokes equations in both x and y directions. The flow assumed turbulent with RNG $k-\varepsilon$ model, since it proved to be more responsive to the effect of rapid strain and streamline curvature, flow separation, reattachment and recirculation. The air at the inlet assumes to follow a power law only in the verification of the work, where the flow assumed uniform, which is the worst case for structural loading [11]. The pressure at the outlet assumed constant with no variation of the velocity components or:

$$\frac{\partial p}{\partial x} = \frac{\partial u}{\partial x} = \frac{\partial v}{\partial x} = 0 \quad (1)$$

The upper line in the study region assumed symmetrical boundary with no-slip at the boundaries of the trough collector and the receiver pipe. The properties of the air assumed constant since the heat transfer process neglected due to small effect of the receiver high temperature on the calculations [4].

International Journal of Innovative Research in Science, Engineering and Technology

(A High Impact Factor, Monthly Peer Reviewed Journal)

Vol. 5, Issue 1, January 2016

III. VERIFICATION OF THE PRESENT WORK AND COMPUTATIONAL WORK:

A full-scale Euro trough solar collector studied in the present work, where the specifications of the trough tabulated in Table 1. The inner and outer diameters of the stainless steel absorber tube are 6.6 cm and 7 cm, respectively. The study domain is a big rectangle of 145 m long and 18 m height. The aperture of the collector is 5.8 m, as shown in figure 1.

The mesh refined around the collector surface, the vertical wall (windbreaker), the HCE near wake and, stretched away from the collector, as shown in figure 2. In order to capture the flow structures near wake of the PTC and around the HCE, mesh requirements are higher in these zones. However, due to the large difference between the dimensions of the aperture of the parabola and the receiver tube, the construction of the mesh is quite dense and complicated near these elements.

The present work solved by using a finite difference method using COMSOL Multiphysics v 5.0 Program solver. The iterative solution considered to converge when the maximum of the residual across all nodes is less than 10^{-6} for continuity, velocities, and temperature.

The numerical results checked for grid independency. The procedure repeated when increasing the number of nodes until a stage reached where the results produce negligible changes with further refinement in grid size. The meshing refined near the trough collector and the windbreaker, and it extra refined near the receiver due to big change in thermal and momentum values.

Validation of the present work obtained by the comparison of the thermal results of [12], where a good agreement shown in Table 2.

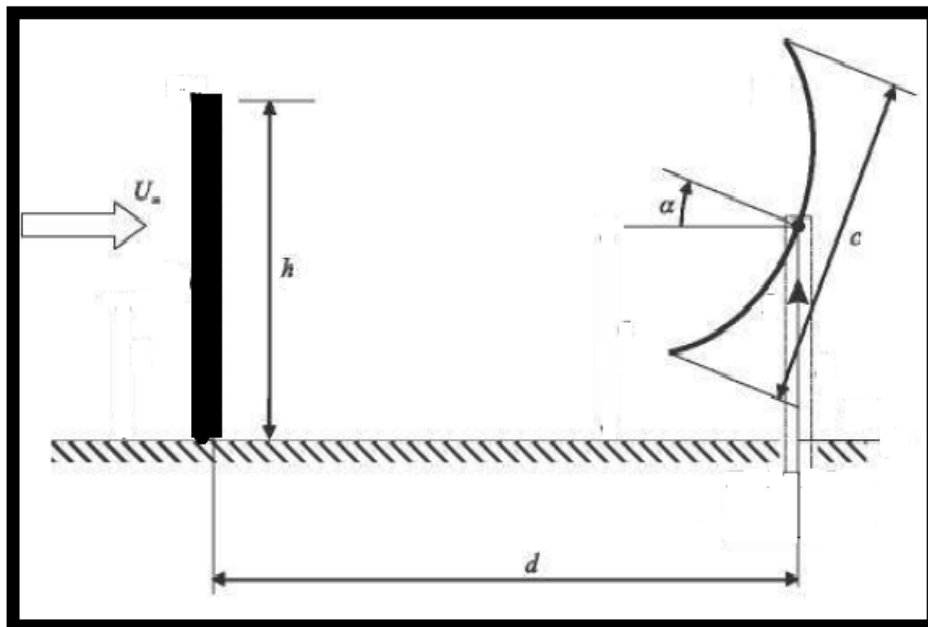


Figure 1 the representation of present work studied.

International Journal of Innovative Research in Science, Engineering and Technology

(A High Impact Factor, Monthly Peer Reviewed Journal)

Vol. 5, Issue 1, January 2016

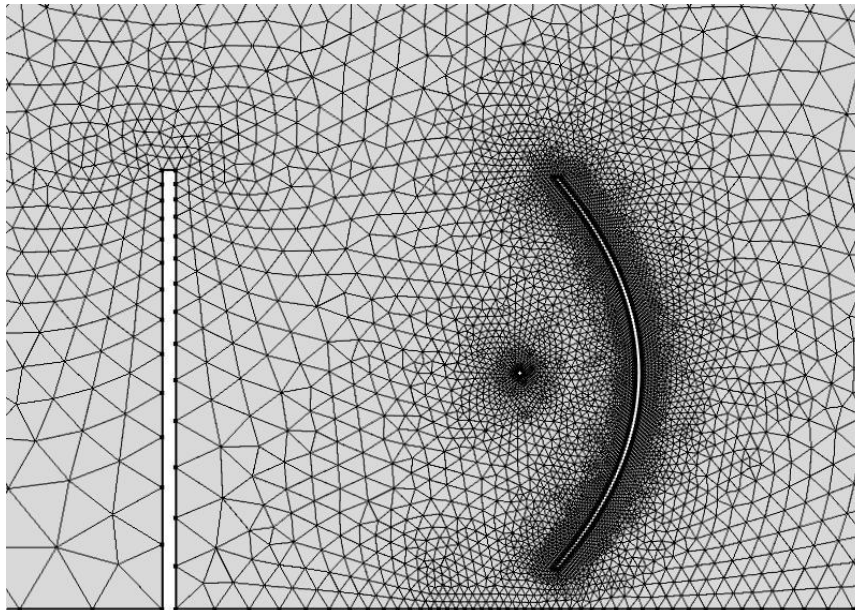


Figure 2 The meshing of the work domain.

IV. RESULTS AND DISCUSSION

Numerical analysis carried out in the region of interest for steady state wind flow over the ground. Convergence of the solution obtained when the residual of the equations reduces less than 10^{-6} .

In figure 3, the velocity contours shown with the streamlines. One case is taken, where the results meant to show the difference in the behavior of the flow with the inlet wind speed. Five different wind speeds of (1, 2.5, 5, 10, and 15 m/s) are taken. The results show no significant change in the behavior, just in the local values, where the streamlines gave the same behavior with each change in wind speed.

In figure 4, the streamlines of the air shown with the change of wind break elevation. The elevations taken are 5.8, 11.6, and 17.4 m, which are equal to c , $2c$, and $3c$ (c is the chord of the trough = 5.8m). The results show that the wind break rises the lowing air up away from the trough, and produce a zone of slow motion zone behind the wind break within over 35m. The slow motion zone increases as the elevation of the wind break increase from up to 70m. It is true that the 17.4m wall is an insignificant elevation, because no one can imagine a wall that height, but it produced here just for calculations.

In figure 5, the streamlines shown with the change in the separation distance between the windbreak and the trough. 5, 15, 35, and 45m separation distance taken. In the first two distances (5, and 15m), the trough shown to in the shadow of the wall, where the motion of the air is very small. The next distances show that the trough is subjected to medium, but still less than the main stream velocity, air motion with a creation of a very big eddies in front of and behind the trough.

One of the most important variables judging the design of troughs is the heat loss to air. Figures 6 and 7 show the results of local Nusselt number versus the change of wind break elevation (figure 6), and the change in the separation distance. The overall values of Nusselt number decrease as the elevation increased. The reason behind this increment is due to decrement in the velocity of air in the vicinity of the receiver tube. So, it is reasonable to notice such decrement. But in the other hand, the values of Nusselt number increased as the separation distance increased. This due to the increment in velocity values as the effect of wind break decrease.

The aerodynamic drag force coefficient presented in figures 8 and 9. Figure 8 shows the variation of the drag force with the change of wind velocity. The results also change with the increase of the separation distance. Results show that

International Journal of Innovative Research in Science, Engineering and Technology

(A High Impact Factor, Monthly Peer Reviewed Journal)

Vol. 5, Issue 1, January 2016

the drag coefficient decreased as the wind velocity increased. The reason behind this behavior may be regarded to the inertia force of the air, where the wind break drives the air away from the trough. This behavior agrees with the literatures as in [9]. Figure 8 also shows the increase in the drag coefficient results increased as the separation distance increased. The reason behind this is that the trough is being far away from the effect of the wind break. But figures 8 (c and d) show a values of drag coefficient over than the ordinary values ($CD=2.3$). This behavior caused due to the subjection of the trough to the concentrated and high velocity bundle of air that flows over the tip of the wind break and falls behind the wall due to gravity.

Figure 9 shows the values of the drag coefficients as the elevation of the wind break changed. The results show that the overall values decreased as the wind break height increased. An interesting value is shown in figure 9 (c), where a negative values of CD are shown. The negative values mean that the force is reversed to the opposite face of the trough (the back of the trough). The big height of the wind break causes a big eddy to form behind that wall. This big eddy is the reason behind this formation of negative drag. This behavior can be noticed clearly in figure 10, where the negative values of pressure is clearly shown.

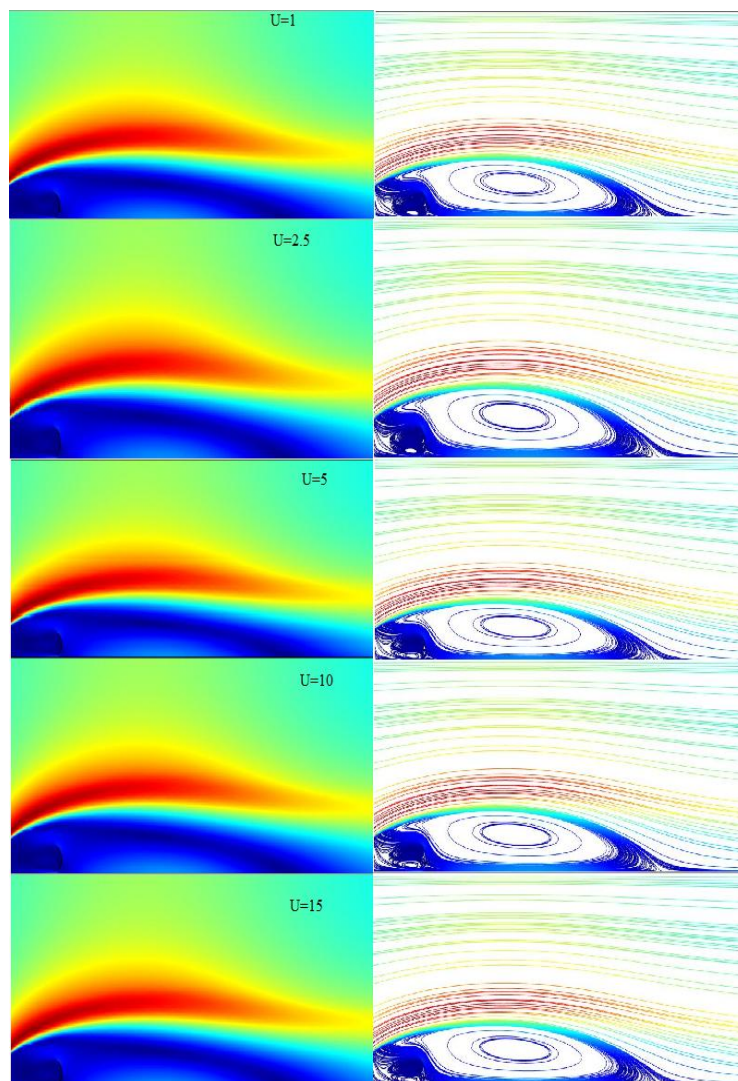


Figure 3 The contours of velocity values to the left and the streamlines to the right with the change of wind velocity.

International Journal of Innovative Research in Science, Engineering and Technology

(A High Impact Factor, Monthly Peer Reviewed Journal)

Vol. 5, Issue 1, January 2016

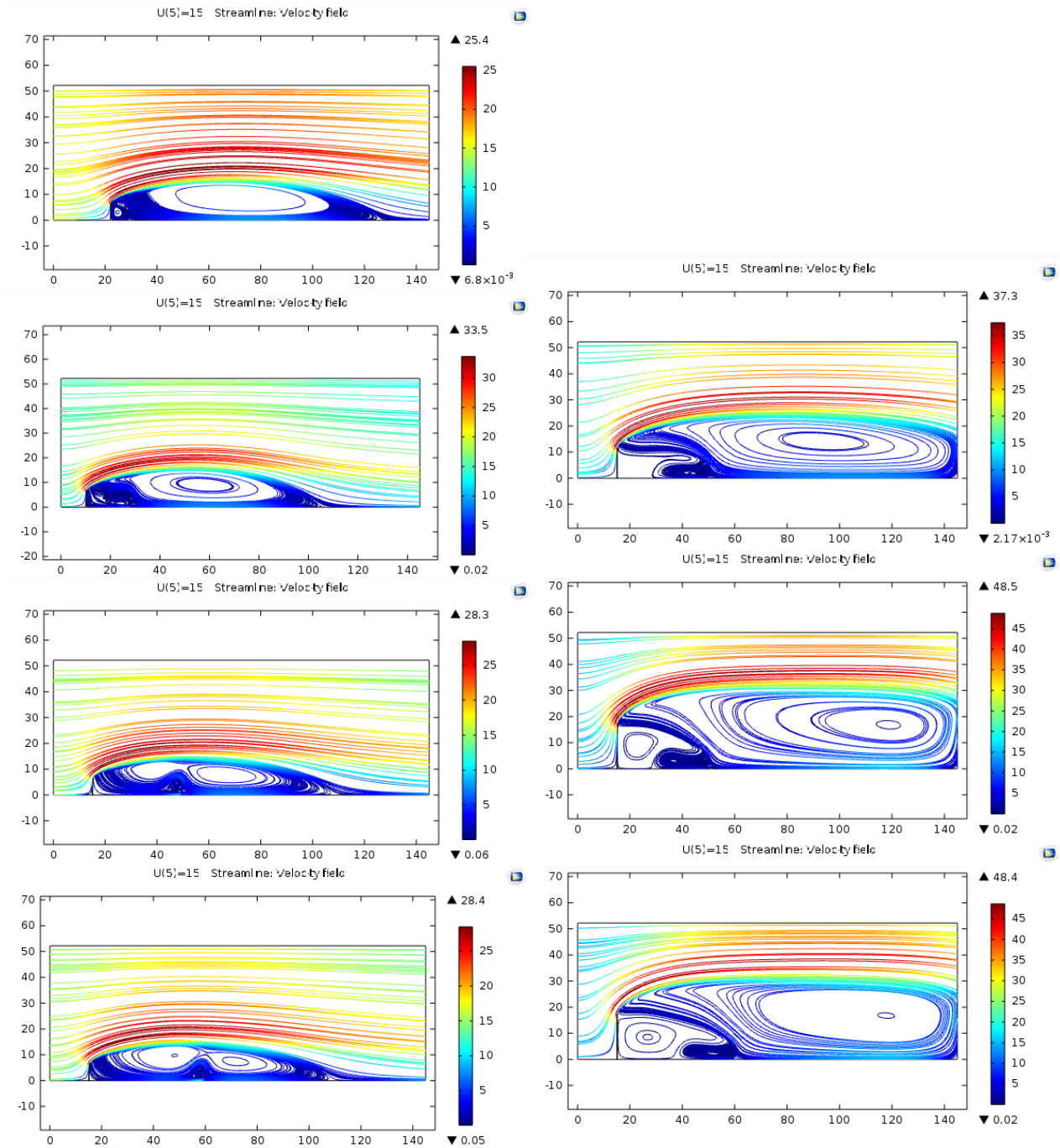


Figure 5 The change of the velocity contours versus the change in windbreak separation distance.

Figure 4 The velocity contours with the change of the windbreak elevation.

International Journal of Innovative Research in Science, Engineering and Technology

(A High Impact Factor, Monthly Peer Reviewed Journal)

Vol. 5, Issue 1, January 2016

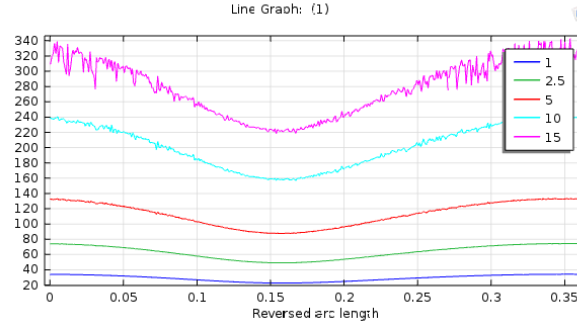
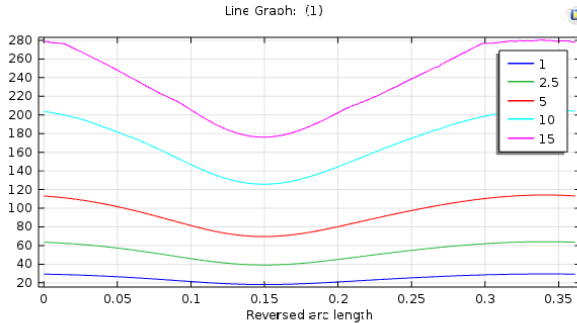
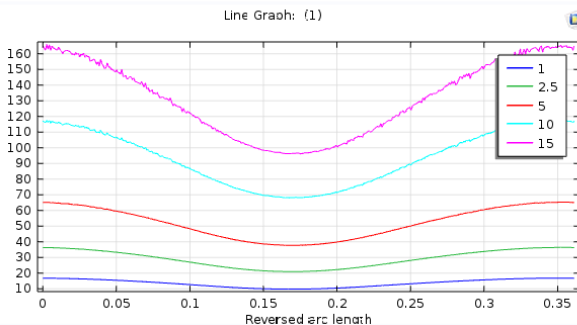
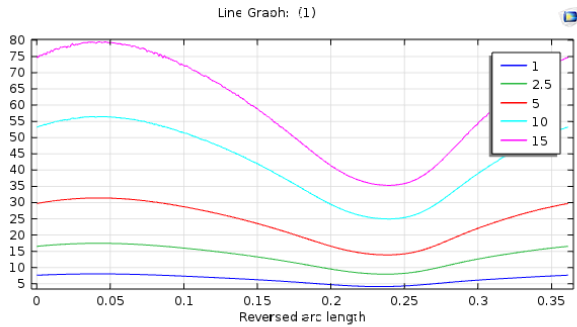


Figure 7 The change of local Nusselt number with different wind velocities and different windbreak separation distance. elevation.

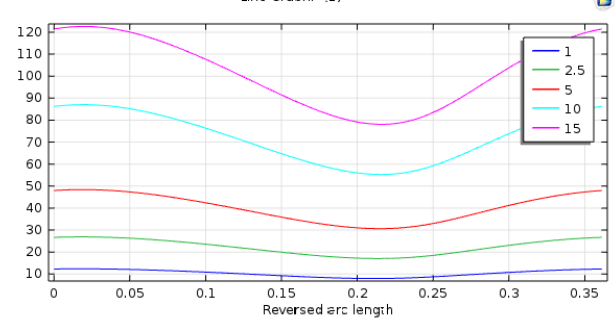
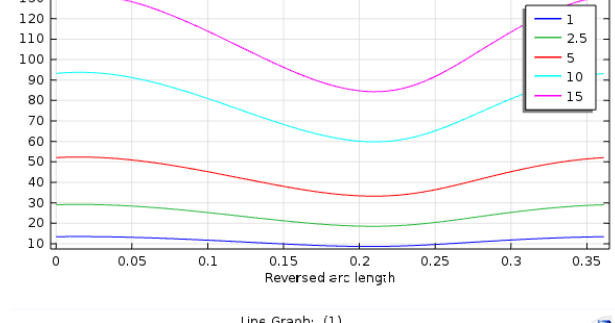
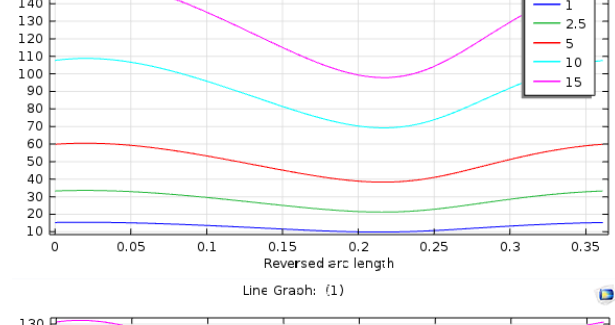
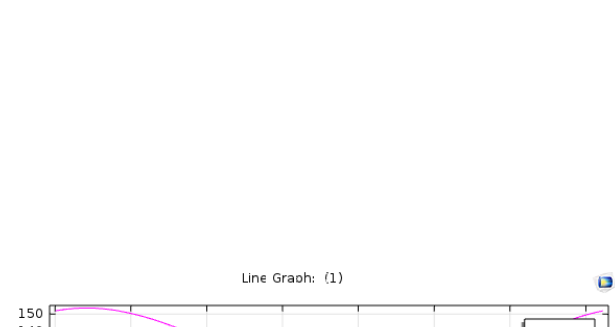


Figure 6 The change of local Nusselt number with different wind velocities and different windbreak elevation.

International Journal of Innovative Research in Science, Engineering and Technology

(A High Impact Factor, Monthly Peer Reviewed Journal)

Vol. 5, Issue 1, January 2016

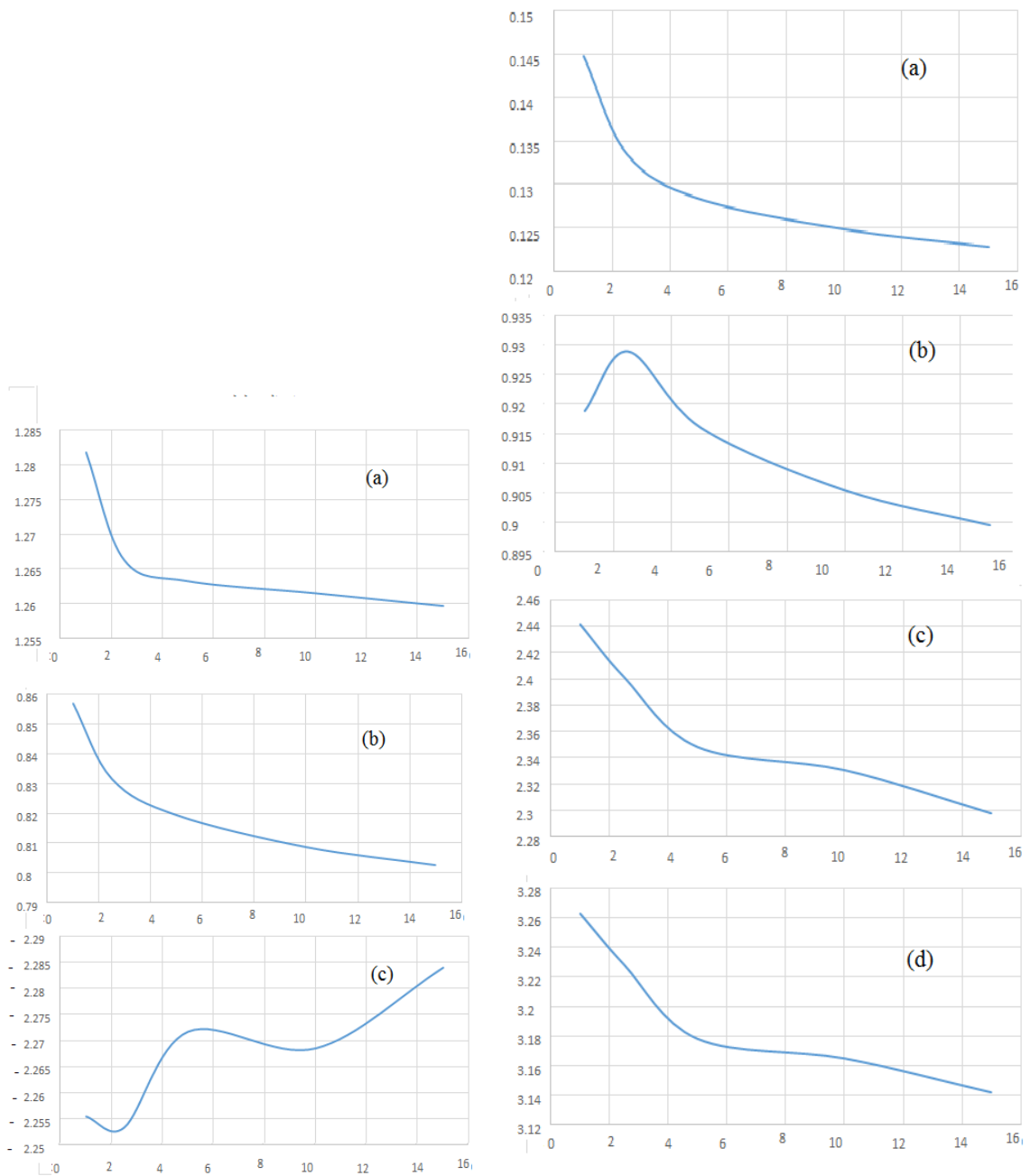


Figure 9 The variation of drag coefficient for different air velocities and the change of air velocities and the change of wind break separation distance.

Figure 8 The variation of drag coefficient for different wind break elevation.

International Journal of Innovative Research in Science, Engineering and Technology

(A High Impact Factor, Monthly Peer Reviewed Journal)

Vol. 5, Issue 1, January 2016

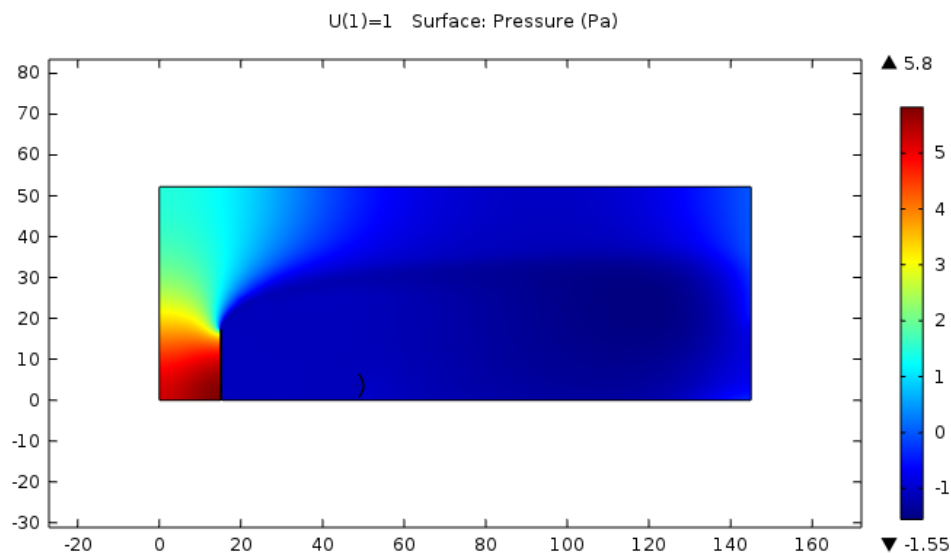


Figure 10 The pressure distribution and the formation of negative pressure.

V. CONCLUSIONS AND RECOMMENDATIONS:

From the previous results, the following remarks can be listed:

The wind break is an efficient method to decrease drag forces on the trough until a certain limit where it become a defect on the process.

- 1- Many troughs can be arranged in the area of the wind shadow.
- 2- The wind break causes a decrease in the heat lost to the environment.
- 3- The elevation increase reverses the value of the drag after a certain limit which should be studied in the future.
- 4- The effect of a row of troughs behind the wind break should be studied.

REFERENCES

- 1- Sadraey M., "Aircraft Performance Analysis", VDM Verlag Dr. Muller, 2009.
- 2- Sun Honghang, et.al, "A Review of Wind Loads on Heliostats and Trough Collectors", Renewable and Sustainable Energy Reviews, 32, pp. 206-221, 2014.
- 3- Murphy L. M., "An Assessment of Existing Studies of Wind Loading on Solar Collectors", Solar Energy Research Institute, 1981.
- 4- Naeeni N., and Yaghoubi M., "Analysis of Wind Flow around a Parabolic Collector (1) Fluid Flow", Renewable Energy, 32, pp. 1898-1916, 2007.
- 5- Garcia E. T., et.al, "On the Effect of Windbreaks on the Aerodynamic Loads over Parabolic Solar Troughs", Applied Energy, vol. 115, pp. 293-300, 2014.
- 6- Gunasena N. U., "An Experimental Study of Mean Wind Forces on Hemispherical Solar Collector", M. Sc. Thesis, Texas Tech University, 1989.
- 7- Hosoya N., et.al, "Wind Tunnel Tests of Parabolic Trough Solar Collectors", Subcontract report, National Renewable Energy Laboratory, 2008.
- 8- Tawfik M. A., et.al, "Study on Wind Loads Coefficients and Flow Field Characteristics around the Parabolic Trough with Stiffeners", Eng., and Tech. Journal, vol. 30, No. 18, 2012.
- 9- Paetzold J., et.al, "Wind Flow around Parabolic Trough Solar Collectors – A Parametric Study for Optimization of Wind Forces and Heat Losses", Proceedings of the 52nd Annual Conference, Australia Solar Energy Society (Australian Solar Council) Melbourne, 2014.
- 10- Murphy L. M., "An Assessment of Existing Studies of Wind Loading on Solar Collector", Report for Solar Energy Research Institute, 1981.
- 11- Daniel, Premjit, et.al, "Numerical investigation of parabolic trough receiver performance with outer vacuum shell", Solar Energy, 85, pp. 1910-1914, 2011.
- 12- Hachicha, A. A., et.al, "Numerical simulation of wind flow around a parabolic trough solar collector", Applied Energy 107, pp. 426–437, 2013.

International Journal of Innovative Research in Science, Engineering and Technology

(A High Impact Factor, Monthly Peer Reviewed Journal)

Vol. 5, Issue 1, January 2016

Table-1: The specification of the Euro trough solar collector (Eckhard Lüpfert and etal, 2001)

Layout	parabolic trough collector
Support structure	steel frame work, pre-galvanized, two variants with light weight, low torsion
Collector length	12 m per element; 100 - 150 m collector length
Drive	hydraulic drive
Max. wind speed	operation: 14 m/s; stow: 40 m/s
Tracking control	Mathematical algorithm + angular encoder checked by sun sensor
Parabola	$y = x^2/4f$ with $f = 1.71$ m
Aperture width (W)	5.8 m
Reflector	28 glass facets per SCE
Absorber tube	evacuated glass envelope, UVAC® or other, application dependent
Fluid	oil, steam, application dependent
Cost	< 200 Euro/m ²

Table 2 The validation datas.

	Position	Nua	Nu _{fsp}	Nu _{max} /Pos	Nu _{min} /Pos
Hachicha, A. A., et.al, 2012	0°	24.5	33.1	41.4/289.5°	9.5/196.8°
Present work	0°	25.8	32.79	34.38/313.7°	10.9/132.5°
Hachicha, A. A., et.al, 2012	90°	47.4	86	86/0°	27.3/222°
Present work	9°	48.3	67.7	69.8/22°	19.99/204.8°
Hachicha, A. A., et.al, 2012	180°	22.5	23.7	29.1/269.5°	7.4/85.9°
Present work	180°	21.66	19.1	25.82/188.8°	15.64/56.3°